

NNLO QCD predictions for the $H \rightarrow WW \rightarrow l\nu l\nu$ signal at the LHC

Charalampos Anastasiou

*PH-Department, CERN
1211 Geneva, Switzerland
E-mail: babis@cern.ch*

Günther Dissertori

*Institute for Particle Physics, ETH Zurich,
8093 Zurich, Switzerland
E-mail: dissertori@phys.ethz.ch*

Fabian Stöckli

*Institute for Particle Physics, ETH Zurich,
8093 Zurich, Switzerland
E-mail: fabstoec@phys.ethz.ch*

ABSTRACT: We present a first computation of the next-to-next-to-leading order (NNLO) QCD cross-section at the LHC for the production of four leptons from a Higgs boson decaying into W bosons. We study the cross-section for a mass value of $M_h = 165$ GeV; around this value a Standard Model Higgs boson decays almost exclusively into W-pairs. We apply all nominal experimental cuts on the final state leptons and the associated jet activity and study the magnitude of higher order effects up to NNLO on all kinematic variables which are constrained by experimental cuts. We find that the magnitude of the higher order corrections varies significantly with the signal selection cuts. As a main result we give the value of the cross-section at NNLO with all selection cuts envisaged for the search of the Higgs boson.

KEYWORDS: QCD, Higgs, LHC Physics, NLO and NNLO Computations.

1. Introduction

The search for the Higgs boson will be one of the major experimental activities at the Large Hadron Collider. The ATLAS and CMS detectors at the LHC are designed to discover a Higgs boson with a mass up to about 1 TeV. The experimental signals of a Higgs boson have been studied in detail during the last years. These studies indicate that a 5σ discovery of a Standard Model (SM) Higgs boson could be possible over the entire mass range with an integrated luminosity of about 30 fb^{-1} (see, for example, [1]).

In the mass regions below $\sim 155\text{ GeV}$ and above $\sim 180\text{ GeV}$ the main detection channels are $H \rightarrow \gamma\gamma$ and $H \rightarrow ZZ \rightarrow 4\ell$, where narrow invariant mass peaks can be reconstructed from isolated photons and leptons. In the region between 155 GeV and 180 GeV the Higgs boson decays almost exclusively into a pair of nearly on-shell W bosons, which subsequently decay to jets or lepton-neutrino pairs.

The discovery of a Higgs boson in this mass range was for a long time regarded as very difficult. The hadronic and semi-leptonic channels are not viable for the discovery because of the overwhelming QCD jet background. The leptonic channel with two isolated charged leptons and large missing transverse energy provides a much cleaner signal, however, because of the undetected neutrinos in the final state no narrow mass peak can be reconstructed. The absence of the latter could be compensated by the large cross-section [2–6] if the dominant backgrounds of non-resonant $pp \rightarrow WW$ and $pp \rightarrow t\bar{t}$ production were reduced significantly. Before any selection cuts are applied, the top-quark background cross-section is about 45 times and the W-pair background cross-section about 6 times larger than the signal cross-section [7]. Good selection criteria to reduce these backgrounds were not found easily; it was believed for some time that a Higgs boson with a mass in this range could remain undetected at the LHC.

In 1996, Dittmar and Dreiner [8] studied the effects of spin correlations and the mass of the resonant and non-resonant WW system. For signal events they observed that the opening angle $\phi_{\ell\ell}$ between the leptons in the plane transverse to the beam axis tends to be small; in addition, the transverse momentum (p_T) spectrum of the charged leptons is somewhat sensitive to the Higgs-boson mass. In contrast, the lepton angle $\phi_{\ell\ell}$ for the background tends to be large and can be used as a discriminating variable. In order to reduce the large top-pair background, which is characterized by strong jet activity, they proposed to reject events where jets have a large p_T . With these basic selection criteria, it has been concluded that a discovery in the channel $H \rightarrow WW \rightarrow \ell\nu\ell\nu$ with $\ell = e, \mu, \tau$ ($\rightarrow \ell\nu\nu$) for a Higgs mass from 155 GeV to 180 GeV is indeed possible [8], even with only a few fb^{-1} of integrated luminosity [7].

The ratio of the Higgs signal cross-section to the cross-section for the background processes after the application of such cuts is estimated to range between 1 : 1 and 2 : 1, depending on the precise value of the Higgs boson mass. The tuning of the selection cuts which leads to these spectacular ratios [7, 8] is based on a thorough analysis of many kinematic distributions for both signal and background processes. The required cross-sections were calculated [9–11] using a leading-order parton shower Monte-Carlo simulation combined with re-weighting methods, in an attempt to effectively incorporate the effects

of higher order QCD corrections [12, 13].

A precise knowledge of the cross-sections and the efficiency of the selection cuts is particularly important in this discovery channel because of two reasons:

(i) The cuts reduce the cross-section for the signal by one order of magnitude and the background by almost three orders of magnitude; a small uncertainty in the efficiency could result in a more significant uncertainty in the signal to background (S/B) ratio.

(ii) Unlike other mass regions where a resonance mass peak can be reconstructed, the measurement of the Higgs boson mass will rely on the precise knowledge of both the signal cross-section and distributions of kinematic observables [9].

The inclusive cross-section for the production of a Higgs boson at the LHC receives large corrections at next-to-leading-order (NLO) [2, 3] and smaller but significant corrections at next-to-next-to-leading-order (NNLO) [4–6] in QCD. It is believed that corrections beyond NNLO are small, as indicated by recently computed leading logarithmic contributions at NNNLO [14, 15] and resummation [16–19].

The computation of differential cross-sections beyond NLO is challenging. The first NNLO differential distribution for a collider process was computed in 2003 [21, 22]. Fully differential cross-sections have appeared soon after and a significant number of new results has been published [23–29]. The cross-section for the production of a Higgs boson via gluon fusion $pp \rightarrow H$ was the first example of such a calculation for a hadron collider process [30]. An application of this result was the NNLO prediction for the di-photon Higgs signal cross-section at the LHC [31]. Recently, a Monte-Carlo program for the same purpose, based on a different method for computing NNLO cross-sections, has been presented in [24].

Comparisons of the NNLO results with those of the event generators PYTHIA and MC@NLO [33–35] for the di-photon signal [12, 32] showed that, in most cases, higher order effects can be well approximated by multiplying the predictions of the generators with the K -factor for the inclusive cross-section. However, the cuts for the di-photon signal are mild and do not alter significantly the shape of kinematic distributions, while the reduction of the Higgs boson cross-section by selection cuts like the ones discussed above is drastic in the $pp \rightarrow H \rightarrow WW \rightarrow \ell\nu\ell\nu$ channel. The distributions of kinematic observables after selection cuts may have very different properties than the corresponding inclusive distributions. An example for this behavior can be found in the study of the jet-veto at NNLO [20, 31]. Additional evidence is shown by re-weighting leading-order Monte-Carlo generator events with K -factors to account for higher order effects in kinematic distributions of the Higgs boson [12, 13]. From these observations it becomes clear that it is essential to compute kinematic distributions of the final-state leptons and the signal cross-section with all experimental cuts applied at NNLO in QCD.

In Ref. [31], the NNLO Monte-Carlo program FEH₁P was published. FEH₁P computes differential cross-sections for Higgs boson production via gluon fusion and includes a selection function for applying experimental cuts on the di-photon final state. In this paper we extend FEH₁P to include the matrix-elements for the decay of the Higgs boson in the $pp \rightarrow H \rightarrow WW \rightarrow \ell\nu\ell\nu$ channel and a selection function for the leptonic final-state. In addition, we have parallelized the evaluation of distinct contributions to the cross-section. The results of our paper comprise kinematic distributions of the final state leptons as well as

the cross-section for $pp \rightarrow H \rightarrow WW \rightarrow \ell\nu\ell\nu$ at next-to-next-leading order of perturbative QCD, taking into account all selection cuts at parton level.

2. The NNLO Monte-Carlo program FEHiP

FEHiP computes phase-space integrals with arbitrary selection cuts and infrared divergences due to unresolved single or double real radiation [29]. The NNLO matrix-elements for Higgs boson production in gluon fusion are rendered numerically integrable, by applying a sector decomposition algorithm [29,36,37], splitting the phase-space into sectors with a simplified infrared structure.

In this paper, we extend FEHiP to the $pp \rightarrow H \rightarrow WW \rightarrow \ell\nu\ell\nu$ decay channel. This requires the decay matrix-elements for $H \rightarrow WW \rightarrow \ell\nu\ell\nu$ and a selection function for the four leptons in the final state.

There are two methods to combine the various sectors into the final result:

(i) We can add up the integrands for all sectors before performing a Monte-Carlo integration; this has the advantage that large cancellations among sectors do not spoil the accuracy of the numerical integration. The drawback of this approach is that each sector exhibits a different singularity structure; the adaptation of the integration to the peaks of the combined integrand is then complicated.

(ii) We can integrate each sector independently and add up the results at the end. The integrands for each sector are now simpler, but large cancellations between positively and negatively valued sectors may spoil the statistical accuracy of the final result.

In Ref. [31] it was found that adding the sectors together before integration resulted in a better performance for a single (not decaying) Higgs boson or the photon pair as final states. In a non-parallel computation (which was sufficient), the alternative to integrate the sectors separately was slow.

In our current calculation, the experimental cuts reject a large part of the total cross-section, and a very good sampling of the phase-space is required. This is prohibitively slow for the sum of the sectors. We have modified FEHiP in order to integrate each sector separately. We have found that the Monte-Carlo adaptation in each sector is excellent. We did not encounter large cancellations among sectors; the cross-sections for individual sectors were usually of the same order of magnitude as the final result.

We have performed a two-fold parallelization of FEHiP. First, each sector is integrated on a dedicated set of independent processor units. Second, each sector may be integrated in parallel on up to 64 CPUs using a program based on the algorithm PVEGAS [39]. The parallelization of sector decomposition for the computation in this paper serves as a successful prototype example for other future applications of the method.

3. Selection cuts and physical parameters

In the following we describe the experimental cuts which we use in our studies. These cuts are required to isolate the Higgs signal from the background, as discussed in the introduction. We keep the values of the cut parameters as close as possible to the ones

described in Refs [7, 9] and in the CMS Physics Technical Design Report [1]. These cuts are motivated by the original study of [8], but are not identical.

As a first selection two isolated leptons (electrons or muons) with opposite charge and high transverse momentum p_T are required. Such leptons mainly originate from decays of electro-weak gauge bosons. In order to reject Drell-Yan Z-production events, these leptons should not be back-to-back in the plane transverse to the beam axis and their invariant mass should be well below the Z mass. Furthermore, some missing transverse energy is required. After applying these selection criteria the remaining sample is dominated by events which contain a pair of charged leptons originating from the decay of Ws, either from the signal or from the main backgrounds. The parameters we consider for this first selection (*pre-selection cuts*) are:

1. both charged leptons should have a transverse momentum of $p_T > 20 \text{ GeV}$ and a pseudorapidity $|\eta| < 2$;
2. the di-lepton mass should be $M_{\ell\ell} < 80 \text{ GeV}$;
3. the missing energy in the event, E_T^{miss} , has to exceed 20 GeV^1 ;
4. the opening angle $\phi_{\ell\ell}$ between the two leptons in the transverse plane should be smaller than 135° .

Following this pre-selection, further kinematic cuts exploit the different dynamics in signal and background : (i) W-pairs from top-quark decays are usually accompanied by jets, therefore a jet-veto can strongly reduce the $t\bar{t}$ background; (ii) spin correlations lead to a small opening angle for signal events, in contrast to the non-resonant W-pair production, and (iii) for the signal the observable lepton transverse momentum spectra show a Jacobian peak-like structure which depends on the Higgs mass.

We consider the following more stringent experimental cuts, which are designed to isolate the Higgs signal (*signal cuts*):

1. the charged leptons should have a transverse momentum of $p_T > 25 \text{ GeV}$ and a pseudorapidity $|\eta| < 2$;
2. these leptons must be isolated from hadrons; the hadronic energy within a cone of $R = 0.4$ around each lepton must not exceed 10% of the corresponding lepton transverse momentum;
3. the di-lepton mass should fall into the range $12 \text{ GeV} < M_{\ell\ell} < 40 \text{ GeV}$. The lower cut reduces potential backgrounds from b-resonances;

¹We compute E_T^{miss} from the momenta of the neutrinos. In a real experiment this variable must be computed differently. One possibility is to compute it by balancing the p_T of the visible leptons. This is a relatively accurate approach when a jet-veto is applied, since it forbids any large jet activity in the central region. We have observed that defining E_T^{miss} from the momenta of the neutrinos or the momenta of the visible leptons yields results which differ by less than 3% at NLO when all other cuts for signal selection are applied.

4. the missing transverse energy in the event, $E_{\text{T}}^{\text{miss}}$, has to exceed 50 GeV;
5. the opening angle $\phi_{\ell\ell}$ between the two leptons in the transverse plane should be smaller than 45° ;
6. there should be no jet with a transverse momentum larger than 25 GeV ² and pseudorapidity $|\eta| < 2.5$. Jets are found using a cone algorithm with a cone size of $R = 0.4$;
7. the harder lepton is required to have $30 \text{ GeV} < p_{\text{T}}^{\text{lept}} < 55 \text{ GeV}$.

In what follows we study a Higgs boson with a mass value $M_h = 165 \text{ GeV}$; the width of the Higgs boson is computed to be 0.254 GeV using the program HDECAY [41]. The Higgs propagator is treated in the narrow width approximation. By comparing with MCFM [42], which includes a Breit-Wigner distribution for the Higgs propagator, we found that at LO and NLO this is accurate within 2%. We have set $M_W = 80.41 \text{ GeV}$ and take into account finite width effects for the W bosons; we set $\Gamma_W = 2.06 \text{ GeV}$. The mass of the top-quark is set to $M_t = 175 \text{ GeV}$. FEHiP calculates the Higgs boson cross-section in the infinite top-quark mass approximation, but the result is normalized to the Born cross-section with the exact top-quark mass dependence (the b-quark contribution to the Born amplitude is neglected). We are using the MRST2001 [43] at LO and the MRST2004 [44] parton distribution functions at NLO and NNLO.

All cross-sections which we present in the rest of the paper, correspond to one final-state lepton combination, e.g. $pp \rightarrow H + X \rightarrow W^+W^- + X \rightarrow e^+e^-\nu\bar{\nu} + X$. In order to obtain the cross-sections for combinations of lepton final-states our results need to be multiplied with a factor 4 for all (e, μ) combinations and with a factor 9 for all (e, μ, τ) combinations ³.

In this work we only study the production of a Higgs boson in gluon fusion, without considering the weak boson fusion process [45, 46]. We also do not consider the effect of electroweak corrections to the production [47] or the decay of the Higgs boson [48]. The process $pp \rightarrow ZZ \rightarrow \ell\nu\ell\nu$ and interference effects will be the subject of a future publication.

In Section 5 we shall present the cross-section for both the *pre-selection cuts* and the *signal cuts*.

4. Magnitude of QCD corrections for kinematic distributions

In this Section we study the cross-section through NNLO, applying a cut on only one kinematic variable at a time. In all plots of this Section, we consider a typical variation of the renormalization (μ_{R}) and factorization scale (μ_{F}) simultaneously, in the range $\frac{M_h}{2} < \mu = \mu_{\text{R}} = \mu_{\text{F}} < 2M_h$. The inclusive cross-section for $pp \rightarrow H + X \rightarrow \ell\nu\ell\nu + X$ is given in Table 1. The K -factors for the inclusive cross-section,

²In [7] a cut on the un-corrected transverse energy and a jet sub-structure parameter are used which corresponds to a jet transverse-energy cut of about 25 GeV.

³We do not consider the decay of the τ leptons.

$\sigma(\text{fb})$	LO	NLO	NNLO
$\mu = \frac{M_h}{2}$	152.63 ± 0.06	270.61 ± 0.25	301.23 ± 1.19
$\mu = 2M_h$	103.89 ± 0.04	199.76 ± 0.17	255.06 ± 0.81

Table 1: The cross-section through NNLO with no experimental cuts applied.

$$K_{(N)NLO}(\mu) = \frac{\sigma_{(N)NLO}(\mu)}{\sigma_{LO}(\mu)}, \quad (4.1)$$

range from 1.77 to 1.92 at NLO and from 1.97 to 2.45 at NNLO, depending on the scale choice ⁴.

It is important to compare the perturbative expansions for the inclusive cross-section and differential Higgs boson observables. We find many kinematic distributions which exhibit a different perturbative pattern than the inclusive cross-section. We present here integrated differential distributions

$$\sigma(X) = \int^X \frac{\partial \sigma}{\partial x} dx;$$

the result for a bin $x \in [X_1, X_2]$ can be obtained from the difference

$$\sigma(x \in [X_1, X_2]) = \sigma(X_2) - \sigma(X_1).$$

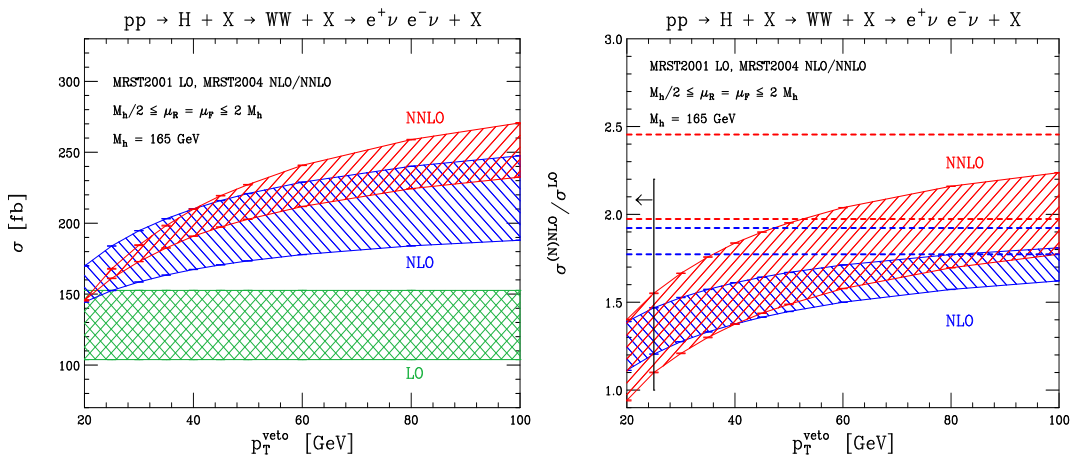


Figure 1: On the left plot, the cross-section to produce a Higgs boson vetoing events with jets in the central region $|\eta| < 2.5$ and $p_T^{\text{jet}} > p_T^{\text{veto}}$ (no other cut is applied). On the right plot, the K -factor as a function of p_T^{veto} . The dashed horizontal lines correspond to the NLO and NNLO K -factors for the inclusive cross-section. The vertical solid line denotes the value of p_T^{veto} in the *signal cuts* of Section 3.

⁴Note that the K -factor is often defined in the literature as the ratio of the NLO or the NNLO cross-section at a scale μ over the LO cross-section at a fixed scale μ_0 (e.g. $\mu_0 = M_h$). Since we allow with our definition in Eq. 4.1 both numerator and denominator to vary, a large scale variation of the K -factor does not necessarily indicate a big scale variation of the NLO or the NNLO cross-section in the numerator.

In Fig. 1 we re-consider the effect of the veto on jets with transverse momentum $p_T^{\text{jet}} > p_T^{\text{veto}}$ (see also [20, 30]). Here, we only veto central jets with rapidity $|\eta| < 2.5$, while all events with jets at larger rapidity are accepted. Jets are defined using a cone algorithm [40] with a cone size $R = 0.4$. We observe that the relative magnitude of the NLO and NNLO contributions depends strongly on p_T^{veto} . The NNLO cross-section increases more rapidly than the NLO by relaxing the veto. Fig. 1 demonstrates that the large NLO and NNLO corrections must be attributed to contributions from jets with large rather than small transverse momentum.

In order to reduce the $pp \rightarrow t\bar{t}$ background, it is required to choose a small value of p_T^{veto} . As we decrease the value of the allowed jet transverse energy, the scale uncertainty at NNLO decreases. At around $p_T^{\text{veto}} = 20 \text{ GeV}$ the difference of the cross-section at $\mu = 2M_h$ and $\mu = \frac{M_h}{2}$ changes sign. In this kinematic region logarithmic contributions $\log(p_T^{\text{veto}})$ from soft radiation beyond NNLO should also be examined [20]. However, the small scale uncertainty at NNLO and the small magnitude of the corrections suggest that such logarithms have a mild effect.

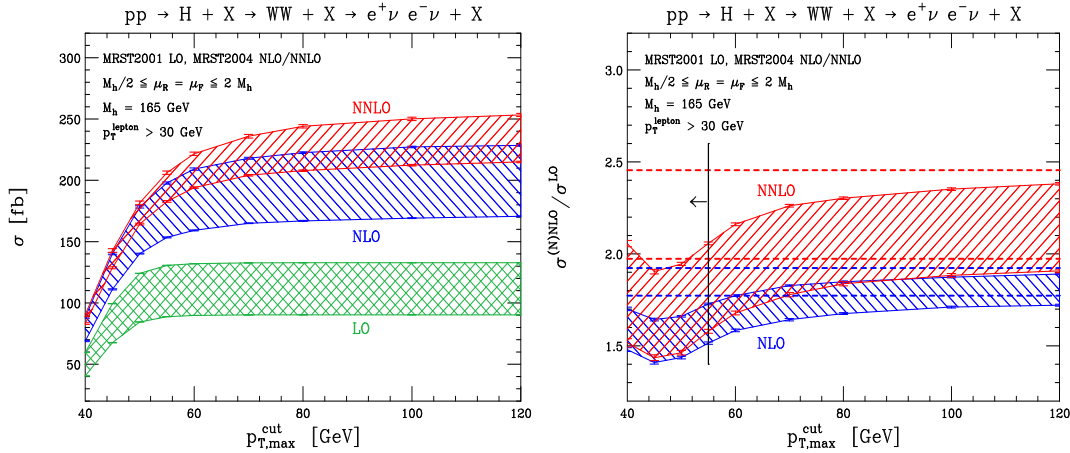


Figure 2: On the left plot, the cross-section for events where the hardest visible lepton has transverse momentum $30 \text{ GeV} < p_T^{\text{lepton}} < p_{T,\max}^{\text{cut}}$. On the right plot, the K -factor as a function of $p_{T,\max}^{\text{cut}}$ (no other cut is applied). The dashed horizontal lines correspond to the NLO and NNLO K -factors for the inclusive cross-section. The vertical solid line denotes the value of $p_{T,\max}^{\text{cut}}$ in the *signal cuts* of Section 3.

In Fig. 2 we show the cross-section after the requirement that the transverse momentum of the hardest visible lepton is restricted to the interval $30 \text{ GeV} < p_T^{\text{lepton}} < p_{T,\max}^{\text{cut}}$. In Ref. [7] the upper boundary of the allowed region was chosen as $p_{T,\max}^{\text{cut}} = 55 \text{ GeV}$. At LO, only $\sim 1\%$ of the hardest visible leptons have transverse momentum of $p_T^{\text{lepton}} > 55 \text{ GeV}$. However, at NLO (NNLO) about ~ 13 (19)% of the events lie above this cut. Thus the choice $p_{T,\max}^{\text{cut}} = 55 \text{ GeV}$ removes regions of the phase-space that are only populated at NLO and NNLO. We observe that the NLO and NNLO K -factors are smaller below this cut. In addition, the scale uncertainty drops below 12% at NNLO, while the corresponding scale uncertainty for the inclusive cross-section is 17%.

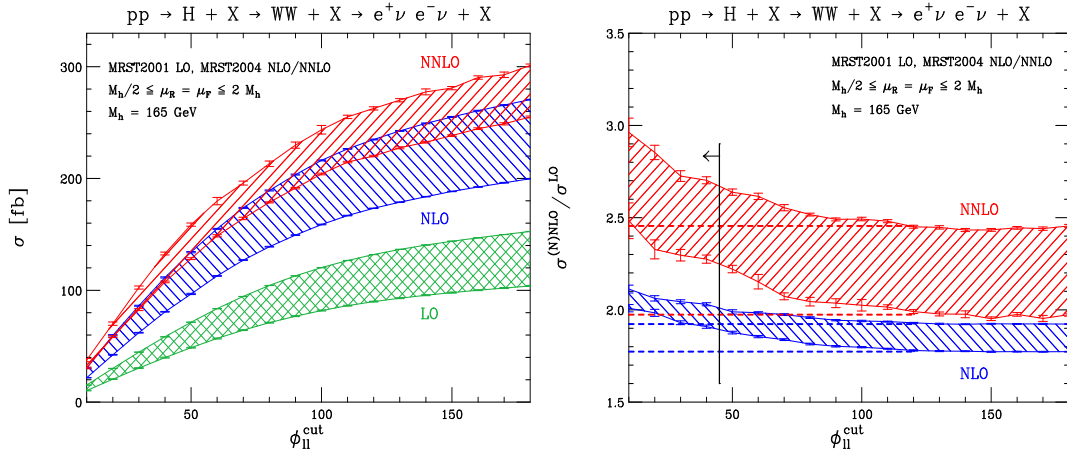


Figure 3: On the left plot, the cross-section for visible leptons with an angle on the transverse plane $\phi_{\ell\ell} < \phi_{\ell\ell}^{\text{cut}}$. On the right plot, the K -factor as a function of $\phi_{\ell\ell}^{\text{cut}}$ (no other cut is applied). The dashed horizontal lines correspond to the NLO and NNLO K -factors for the inclusive cross-section. The vertical solid line denotes the value of $\phi_{\ell\ell}^{\text{cut}}$ in the *signal cuts* of Section 3.

A powerful discriminating variable between the signal and the $pp \rightarrow WW$ background is the opening angle $\phi_{\ell\ell}$ between the two visible leptons in the plane transverse to the beam axis. In Fig. 3 we plot the cross-section for events with $\phi_{\ell\ell} < \phi_{\ell\ell}^{\text{cut}}$ ⁵. We observe that the NLO and especially the NNLO corrections are significantly larger for small angles $\phi_{\ell\ell}$. For $\phi_{\ell\ell}^{\text{cut}} = 40^\circ$ the NNLO K -factor is ~ 2.27 (2.70) for $\mu = \frac{M_h}{2}$ ($2M_h$). The corresponding K -factor for the inclusive cross-section is ~ 1.97 (2.45). The NNLO scale uncertainty for $\phi_{\ell\ell}^{\text{cut}} = 40^\circ$ is 18.5%, while for the inclusive cross-section it is $\sim 17\%$. Thus the envisaged cut at $\phi_{\ell\ell}^{\text{cut}} \sim 45^\circ$ enhances contributions with large perturbative corrections.

The decay of the W bosons produces large missing transverse energy, E_T^{miss} . In Fig 4 we plot the cross-section for $E_T^{\text{miss}} > E_{T,\text{miss}}^{\text{cut}}$. At leading order, there are no contributions from $E_T^{\text{miss}} > M_W$. This region of the phase-space requires that the Higgs system is boosted with additional radiation at NLO and NNLO. The contribution from $E_T^{\text{miss}} > 80$ GeV, for $\mu = \frac{M_h}{2}$, amounts to 0.7% at LO, $\sim 14\%$ at NLO and $\sim 16\%$ at NNLO. The scale variation for this region of the phase-space is 60% at NLO (essentially LO) and 49% at NNLO (essentially NLO). By requiring very large missing transverse energy, we enhance the significance of the above phase-space region; the K -factors tend to increase with respect to the inclusive cross-section.

In Fig. 5 we plot the cross-section for events with a lepton invariant mass in the interval $12 \text{ GeV} < M_{\ell\ell} < M_{\ell\ell}^{\text{cut}}$. We notice that the cross-section has a perturbative convergence with K -factors and scale variation very similar to the ones for the inclusive cross-section for all choices of $M_{\ell\ell}^{\text{cut}}$.

We have now studied the kinematic behavior of the cross-section through NNLO for all variables which are subject to significant experimental cuts in order to optimize the signal

⁵We note that the distribution of the opening angle at NNLO, using the code of [24], has been presented at the Les Houches workshop in June 2007 [49]. Qualitatively our results are similar.

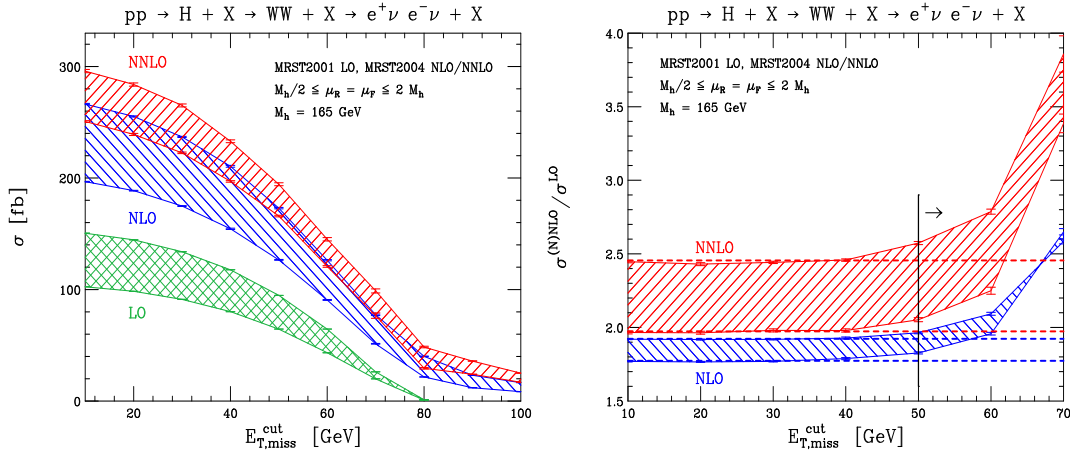


Figure 4: On the left plot, the cross-section for events with missing transverse energy $E_T^{\text{miss}} > E_{T,\text{miss}}^{\text{cut}}$, where E_T^{miss} is computed as the transverse momentum of the neutrino pair. On the right plot, the K -factor as a function of $E_{T,\text{miss}}^{\text{cut}}$ (no other cut is applied). The dashed horizontal lines correspond to the NLO and NNLO K -factors for the inclusive cross-section. The vertical solid line denotes the value of $E_{T,\text{miss}}^{\text{cut}}$ in the *signal cuts* of Section 3.

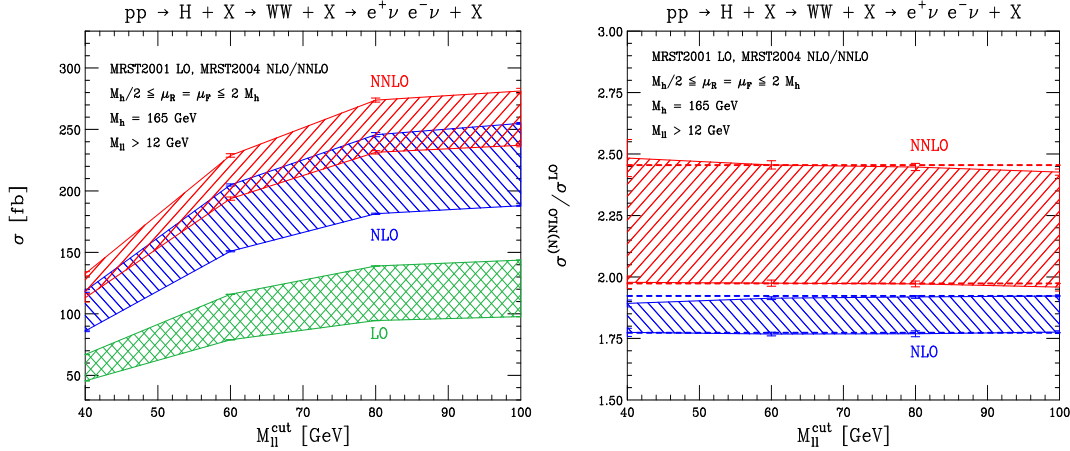


Figure 5: On the left plot, the cross-section for events with visible lepton invariant mass $12 \text{ GeV} < M_{\ell\ell} < M_{\ell\ell}^{\text{cut}}$. On the right plot, the K -factor as a function of $M_{\ell\ell}^{\text{cut}}$ (no other cut is applied). The dashed horizontal lines correspond to the NLO and NNLO K -factors for the inclusive cross-section.

to background ratio. A geometrical cut on isolating the leptons from hadrons (partons in our case) rejects very few events ($\sim 1 - 2\%$).

We have found that the cuts discussed above can change individually the K -factors and the scale variation of the cross-section. In the next Section we will compute the cross-section after applying all the cuts which are described in Section 3.

5. Signal cross-section at the LHC

We present now the main results of our paper, which are the cross-sections for the experimental cuts and parameters of Section 3.

In Table 2 we show the cross-section for the *pre-selection* cuts, which do not impose a jet-veto, for three choices of $\mu_R = \mu_F = \mu$:

The scale variation is $\sim 37\%$ at LO, $\sim 30\%$ at NLO, and $\sim 17\%$ at NNLO. This is a

$\sigma(\text{fb})$	LO	NLO	NNLO
$\mu = \frac{M_h}{2}$	71.63 ± 0.07	126.95 ± 0.13	140.73 ± 0.45
$\mu = M_h$	59.40 ± 0.06	108.42 ± 0.15	130.01 ± 0.36
$\mu = 2M_h$	49.56 ± 0.05	94.33 ± 0.13	119.28 ± 0.26

Table 2: Cross-section through NNLO for the *pre-selection cuts* of Section 3.

similar scale-variation as for the inclusive cross-section in Table 1. The K -factors for the accepted cross-section are also very similar to the K -factors for the inclusive cross-section. The *pre-selection cuts* affect only mildly the perturbative convergence of the cross-section.

We find a very different behavior when the *signal cuts* are applied (Table 3). We

$\sigma(\text{fb})$	LO	NLO	NNLO
$\mu = \frac{M_h}{2}$	21.002 ± 0.021	22.47 ± 0.11	18.45 ± 0.54
$\mu = M_h$	17.413 ± 0.017	21.07 ± 0.11	18.75 ± 0.37
$\mu = 2M_h$	14.529 ± 0.014	19.50 ± 0.10	19.01 ± 0.27

Table 3: Cross-section through NNLO for the *signal cuts* of Section 3.

observe that the NLO and NNLO K -factors are small in comparison to the corresponding K -factors for the inclusive cross-section. The relative magnitude of the NLO and NNLO corrections with respect to LO is similar to the observed K -factors in Fig. 1 for a jet-veto value around ~ 20 GeV. In addition, the scale variation is also small at NNLO (of similar magnitude as the statistical error of our numerical integration); this is again similar to the pattern observed in Fig. 1 for small values of the jet-veto.

The jet-veto enhances the significance of soft gluon radiation and a resummation of large logarithms may be necessary. We investigate the dependence of the cross-section on the jet-veto in Fig. 6, where we have computed the cross-section with all *signal cuts* of Section 3 and for different values of the jet-veto p_T^{veto} . We find that the signal cross-section at NNLO and a jet-veto value $p_T^{\text{veto}} = 40$ GeV is only 13% larger than the cross-section for $p_T^{\text{veto}} = 25$ GeV when $\mu_R = \mu_F = \frac{M_h}{2}$. If we do not apply any other cuts except the jet-veto, the corresponding increase is almost double $\sim 25\%$. Therefore, we conclude that both the jet-veto and the other cuts constrain central jets to low transverse momentum.

The cross-section in Table 3 for the *signal cuts* demonstrates a much better perturbative behavior than the inclusive cross-section. However, before we conclude that we have obtained a very precise prediction for the signal cross-section we would like to investigate

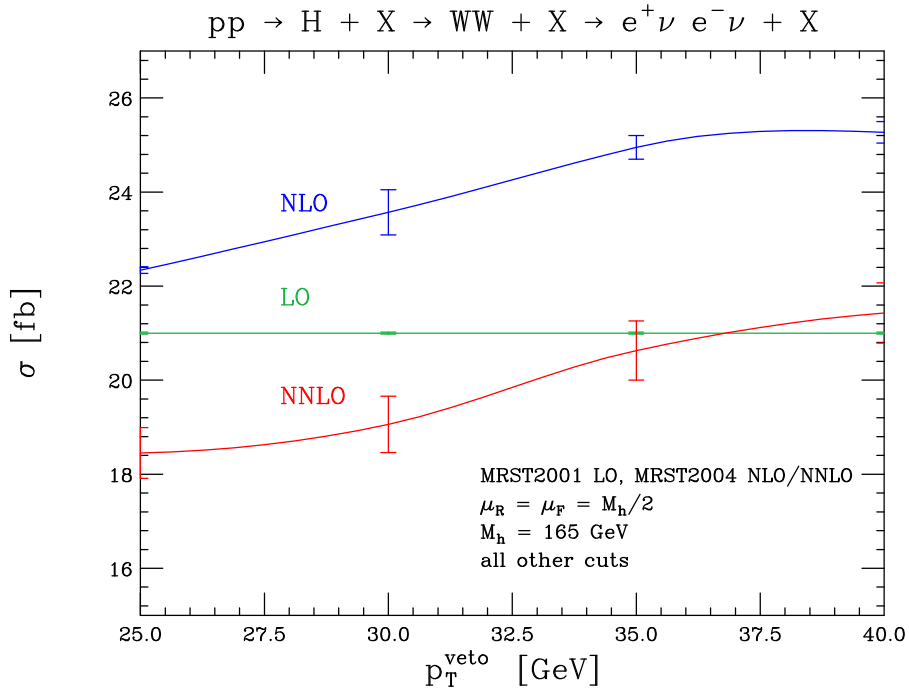


Figure 6: The cross-section for the *signal cuts* varying the value of the jet-veto. The increase in the cross-section by relaxing the jet-veto is slower than in Fig. 1. Other cuts in addition to the jet-veto restrict the p_T of central jets to small values.

further the importance of resummation effects. We computed the average transverse momentum of the Higgs boson to be $\langle p_T^H \rangle_{\text{cuts}} \sim 15$ GeV at NNLO for $\mu_F = \mu_R = \frac{M_h}{2}$. The corresponding average for the inclusive cross-section is $\langle p_T^H \rangle \sim 48$ GeV. Logarithms $\log(p_T^H)$ could therefore have a larger impact on the accepted cross-section with the *signal cuts* than the inclusive cross-section.

The existence of large logarithmic corrections is not manifest by varying the renormalization and factorization scales as shown in Table 3. To investigate this aspect thoroughly, we compute in Table 4 the cross-section with the *signal cuts* of Section 3 for independent values of μ_R and μ_F in the interval $[\frac{M_h}{4}, 2M_h]$. The scale variation in this interval is rather small. We note that the corresponding scale variation for the inclusive cross-section in the smaller interval $[\frac{M_h}{2}, 2M_h]$ is $\sim 17\%$.

We can quantify the effect of p_T logarithms and the need for resummation comparing our NLO and NNLO predictions with the prediction from the parton-shower generator MC@NLO [35, 50]. A comparison of the accepted cross-sections with the cuts of Section 3 is not immediately possible, since the spin correlations in the $H \rightarrow WW \rightarrow \ell\nu\ell\nu$ decay are not treated fully in HERWIG [34]. However, a similar comparison has been made in [12] for the Higgs boson cross-section when only a jet-veto is applied at $p_T^{\text{veto}} = 30$ GeV. It was found that the MC@NLO result is $\sim 26\%$ smaller than the NLO. The NNLO result is smaller than NLO by only about $\sim 9\%$. If one normalizes the MC@NLO to the NNLO inclusive cross-section, the accepted cross-sections for MC@NLO and NNLO after the jet-

$\sigma(\text{fb})$	$\mu_{\text{F}} = \frac{M_h}{4}$	$\mu_{\text{F}} = \frac{M_h}{2}$	$\mu_{\text{F}} = M_h$	$\mu_{\text{F}} = 2M_h$
$\mu_{\text{R}} = 2M_h$	17.89 ± 0.27	18.27 ± 0.29	18.97 ± 0.29	19.01 ± 0.27
$\mu_{\text{R}} = M_h$	18.68 ± 0.90	18.33 ± 0.40	18.75 ± 0.37	19.87 ± 0.42
$\mu_{\text{R}} = \frac{M_h}{2}$	18.84 ± 0.60	18.45 ± 0.54	17.52 ± 0.93	18.10 ± 0.63
$\mu_{\text{R}} = \frac{M_h}{4}$	16.82 ± 0.94	18.40 ± 1.00	16.06 ± 0.94	15.45 ± 0.98

Table 4: NNLO cross-section for the *signal cuts* and independent values of the renormalization scale μ_{R} and the factorization scale μ_{F} .

veto are close; it was found in [12] that the MC@NLO efficiency is $\sim 51\%$, while the NNLO efficiency is $\sim 54\%$. We note that the effect of resummation in comparison to NLO calculations for $pp \rightarrow H \rightarrow WW$ has been studied in [51], however the cuts applied there did not include a jet-veto.

Our NNLO result, which is very close to NLO, exhibits a remarkable stability with varying the renormalization and factorization scales; this alludes, without proving it, to small numerical coefficients of logarithmic terms. In addition, in the presence of the jet-veto only, the MC@NLO and NNLO efficiencies are not very different suggesting that the NNLO result has captured to a large extend the effect of low p_{T} radiation. In a hypothetical ‘‘MC@NNLO’’ calculation the difference to our NNLO result could be even smaller. However, in order to verify this intuition, a better understanding of resummation effects in the presence of all experimental cuts is indispensable.

It is interesting to investigate whether a ‘‘loosening’’ of the experimental cuts could alter the perturbative behavior of the cross-section. Changes in the experimental cuts influence the background cross-sections more significantly than the signal cross-section. Given the complexity of the combined background $pp \rightarrow t\bar{t}$ and $pp \rightarrow WW$ processes, it appears to us that there is little freedom for major changes without spoiling the estimated S/B ratio in [9]. We apply the following changes to the *signal cuts* of Section 3:

- apply a less restrictive jet-veto $p_{\text{T}}^{\text{veto}} = 35 \text{ GeV}$;
- require smaller $E_{\text{T}}^{\text{miss}} > 45 \text{ GeV}$;
- allow a larger lepton invariant mass $12 \text{ GeV} < M_{\ell\ell} < 45 \text{ GeV}$;
- allow larger lepton angles $\phi_{\ell\ell} < 60^\circ$;
- do not restrict the upper value of the p_{T} of the hardest lepton, $p_{\text{T}}^{\text{lepton}} > 30 \text{ GeV}$.

For these new cuts the average momentum of the Higgs boson is only by little larger, $\langle p_{\text{T}}^{\text{H}} \rangle \sim 18 \text{ GeV}$. We find the new cross-section in Table 5. We find once again very small NNLO corrections with respect to the NLO cross-section. The scale variation is very small and remains comparable to our Monte-Carlo integration error.

The NNLO K -factor for the cross-section with the *signal cuts* of Table 3 is $0.9 - 1.3$ depending on the scale choices. One must be careful if this K -factor is applied to rescale the result of a leading order parton-shower generator. At LO in fixed order perturbation

$\sigma(\text{fb})$	LO	NLO	NNLO
$\mu = \frac{M_h}{2}$	28.811 ± 0.028	35.81 ± 0.22	32.48 ± 0.52
$\mu = M_h$	23.884 ± 0.023	32.53 ± 0.16	31.59 ± 0.38
$\mu = 2M_h$	19.933 ± 0.019	29.53 ± 0.15	31.45 ± 0.26

Table 5: Cross-section through NNLO for *loose signal cuts*.

theory, all events have Higgs $p_T = 0$; a jet-veto has a 100% efficiency. Parton-shower event generators produce an extended p_T spectrum, and have a significantly smaller efficiency; for example, the efficiency of Pythia [33] with a jet-veto at $p_T^{\text{veto}} = 30 \text{ GeV}$ is about 50% [12]. The appropriate factor for re-weighting LO event generators is:

$$K_{\text{NNLO}} \times \frac{\text{efficiency(LO)}}{\text{efficiency(MC)}}$$

This factor yields qualitatively similar results as in Refs [12, 13]. However, we have not yet made a consistent comparison of our NNLO result for the signal cross-section and existing predictions from studies based on re-weighting [12, 13].

6. Conclusions

We have performed a first calculation of kinematic distributions and the cross-section with experimental cuts in NNLO QCD for the process $pp \rightarrow H \rightarrow WW \rightarrow \ell\nu\ell\nu$. For this purpose, we have extended the Monte-Carlo program FEH1P [31], by including the matrix-elements for the decay of the Higgs boson and parallelizing the evaluation of sectors [38].

We have observed that many kinematic distributions exhibit K -factors and scale variations which are qualitatively different than in the inclusive cross-section. As a consequence, only when mild (*pre-selection*) cuts are applied the cross-section receives large perturbative corrections through NNLO as for the inclusive cross-section. In contrast, for the selection cuts which are designed to isolate the Higgs boson signal from the background, we find small NNLO corrections and a very good stability with varying the renormalization and factorization scales.

The experimental cuts restrict the phase-space to events with small transverse momentum for the Higgs boson. The effect of resummation should be investigated thoroughly in future works. However, large logarithms do not become manifest when varying the renormalization and factorization scales, and the efficiencies at NNLO and MC@NLO for a typical jet-veto cut differ by less than 6%.

We find that the NNLO K -factors for the signal cross-section after the application of selection cuts are very different than the K -factor for the inclusive cross-section. When the NNLO K -factors, which we have computed here, are used to re-weight leading order event generators, the large ratio between the efficiencies of the fixed order LO result and the prediction of the generators should also be taken into account.

Acknowledgements

We are grateful to Alejandro Daleo, Michael Dittmar and Giulia Zanderighi for discussions and very important observations. We thank Bryan Webber for his comments and communications about the MC@NLO and HERWIG event generators. We thank Giovanna Davatz for communicating to us research in her Ph.D thesis and collaboration on an earlier related project. We are grateful to Thomas Gehrmann, Michele della Morte, Filip Moortgat and Thomas Punz for their help in securing adequate computing resources and useful discussions. CA is grateful to Kirill Melnikov and Frank Petriello for a fruitful collaboration in writing the FEHiP program. We thank the groups of theoretical physics at the University of Zürich and at ETH Zürich for providing computing resources to us. This research was supported in part by the Swiss National Science Foundation (SNF) under the contract 200020-113378/1.

References

- [1] CMS physics: Technical Design Report, CERN-LHCC-2006-021; CMS-TDR-008-2, <http://cmsdoc.cern.ch/cms/cpt/tdr/>
- [2] M. Spira, A. Djouadi, D. Graudenz and P. M. Zerwas, Nucl. Phys. B **453**, 17 (1995) [arXiv:hep-ph/9504378].
- [3] S. Dawson, Nucl. Phys. B **359**, 283 (1991).
- [4] R. V. Harlander and W. B. Kilgore, Phys. Rev. Lett. **88**, 201801 (2002) [arXiv:hep-ph/0201206].
- [5] C. Anastasiou and K. Melnikov, Nucl. Phys. B **646**, 220 (2002) [arXiv:hep-ph/0207004].
- [6] V. Ravindran, J. Smith and W. L. van Neerven, Nucl. Phys. B **665**, 325 (2003) [arXiv:hep-ph/0302135].
- [7] G. Davatz, M. Dittmar, A.-S. Giolo-Nicollerat, CMS Note 2006/047
- [8] M. Dittmar and H. K. Dreiner, Phys. Rev. D **55**, 167 (1997) [arXiv:hep-ph/9608317].
- [9] G. Davatz, M. Dittmar and F. Pauss, arXiv:hep-ph/0612099.
- [10] G. Davatz, M. Dittmar and A. S. Giolo-Nicollerat, J. Phys. G **33**, N85 (2007).
- [11] G. Davatz, A. S. Giolo-Nicollerat and M. Zanetti, CERN-CMS-NOTE-2006-048.
- [12] G. Davatz, F. Stöckli, C. Anastasiou, G. Dissertori, M. Dittmar, K. Melnikov and F. Petriello, JHEP **0607**, 037 (2006) [arXiv:hep-ph/0604077].
- [13] G. Davatz, G. Dissertori, M. Dittmar, M. Grazzini and F. Pauss, JHEP **0405**, 009 (2004) [arXiv:hep-ph/0402218].
- [14] S. Moch and A. Vogt, Phys. Lett. B **631**, 48 (2005) [arXiv:hep-ph/0508265].
- [15] V. Ravindran, Nucl. Phys. B **752**, 173 (2006) [arXiv:hep-ph/0603041].
- [16] G. Bozzi, S. Catani, D. de Florian and M. Grazzini, arXiv:0705.3887 [hep-ph].
- [17] S. Catani, D. de Florian, M. Grazzini and P. Nason, JHEP **0307**, 028 (2003) [arXiv:hep-ph/0306211].

- [18] A. Kulesza, G. Sterman and W. Vogelsang, Phys. Rev. D **69**, 014012 (2004) [arXiv:hep-ph/0309264].
- [19] V. Ravindran, J. Smith and W. L. van Neerven, arXiv:hep-ph/0608308.
- [20] S. Catani, D. de Florian and M. Grazzini, JHEP **0201**, 015 (2002) [arXiv:hep-ph/0111164].
- [21] C. Anastasiou, L. J. Dixon, K. Melnikov and F. Petriello, Phys. Rev. Lett. **91**, 182002 (2003) [arXiv:hep-ph/0306192].
- [22] C. Anastasiou, L. J. Dixon, K. Melnikov and F. Petriello, Phys. Rev. D **69**, 094008 (2004) [arXiv:hep-ph/0312266].
- [23] A. Gehrmann-De Ridder, T. Gehrmann, E. W. N. Glover and G. Heinrich, arXiv:0707.1285 [hep-ph].
- [24] S. Catani and M. Grazzini, arXiv:hep-ph/0703012.
- [25] K. Melnikov and F. Petriello, Phys. Rev. D **74**, 114017 (2006) [arXiv:hep-ph/0609070].
- [26] K. Melnikov and F. Petriello, Phys. Rev. Lett. **96**, 231803 (2006) [arXiv:hep-ph/0603182].
- [27] C. Anastasiou, K. Melnikov and F. Petriello, arXiv:hep-ph/0505069.
- [28] S. Weinzierl, Phys. Lett. B **644**, 331 (2007) [arXiv:hep-ph/0609021].
- [29] C. Anastasiou, K. Melnikov and F. Petriello, Phys. Rev. Lett. **93**, 032002 (2004) [arXiv:hep-ph/0402280].
- [30] C. Anastasiou, K. Melnikov and F. Petriello, Phys. Rev. Lett. **93**, 262002 (2004) [arXiv:hep-ph/0409088].
- [31] C. Anastasiou, K. Melnikov and F. Petriello, Nucl. Phys. B **724**, 197 (2005) [arXiv:hep-ph/0501130], <http://www.phys.hawaii.edu/~kirill/FEHiP.htm>.
- [32] F. Stöckli, A. G. Holzner and G. Dissertori, JHEP **0510**, 079 (2005) [arXiv:hep-ph/0509130].
- [33] T. Sjostrand, L. Lonnblad and S. Mrenna, arXiv:hep-ph/0108264.
- [34] G. Corcella *et al.*, arXiv:hep-ph/0210213.
- [35] S. Frixione and B. R. Webber, JHEP **0206**, 029 (2002) [arXiv:hep-ph/0204244]; arXiv:hep-ph/0612272.
- [36] T. Binoth and G. Heinrich, Nucl. Phys. B **585**, 741 (2000) [arXiv:hep-ph/0004013].
- [37] A. Gehrmann-De Ridder, T. Gehrmann and G. Heinrich, Nucl. Phys. B **682**, 265 (2004) [arXiv:hep-ph/0311276].
- [38] C. Anastasiou, K. Melnikov and F. Petriello, Phys. Rev. D **69**, 076010 (2004) [arXiv:hep-ph/0311311].
- [39] Richard Kreckel, arXiv:physics/9710028; arXiv:physics/9812011.
- [40] G. Sterman and S. Weinberg, Phys. Rev. Lett. **39**, 1436 (1977).
- [41] A. Djouadi, J. Kalinowski and M. Spira, Comput. Phys. Commun. **108**, 56 (1998) [arXiv:hep-ph/9704448].
- [42] J. M. Campbell and R. K. Ellis, Phys. Rev. D **62**, 114012 (2000) [arXiv:hep-ph/0006304] <http://mcfm.fnal.gov/>.

- [43] A. D. Martin, R. G. Roberts, W. J. Stirling and R. S. Thorne, Phys. Lett. B **531**, 216 (2002) [arXiv:hep-ph/0201127].
- [44] A. D. Martin, R. G. Roberts, W. J. Stirling and R. S. Thorne, Phys. Lett. B **604**, 61 (2004) [arXiv:hep-ph/0410230].
- [45] D. L. Rainwater and D. Zeppenfeld, Phys. Rev. D **60**, 113004 (1999) [Erratum-ibid. D **61**, 099901 (2000)] [arXiv:hep-ph/9906218].
- [46] T. Figy, C. Oleari and D. Zeppenfeld, Phys. Rev. D **68**, 073005 (2003) [arXiv:hep-ph/0306109].
- [47] G. Degrossi and F. Maltoni, Phys. Lett. B **600**, 255 (2004) [arXiv:hep-ph/0407249].
- [48] A. Bredenstein, A. Denner, S. Dittmaier and M. M. Weber, JHEP **0702**, 080 (2007) [arXiv:hep-ph/0611234].
- [49] M. Grazzini, <http://wwwlapp.in2p3.fr/conferences/LesHouches/Houches2007/talks/Session2-1/LHHiggsTH.pdf>
- [50] S. Frixione, E. Laenen, P. Motylinski and B. R. Webber, JHEP **0704**, 081 (2007) [arXiv:hep-ph/0702198].
- [51] Q. H. Cao and C. R. Chen, arXiv:0704.1344 [hep-ph].